Reconfigurable RF Impedance Tuner for Match Control in Broadband Wireless Devices

Richard B. Whatley, Zhen Zhou, and Kathleen L. Melde, *Senior Member, IEEE*

***Abstract*—This paper presents the design of a broadband RF impedance tuner that is part of a dynamically reconfigurable automatic match control (AMC) circuit that can be used for a wide variety of wireless devices and intelligent RF front ends. The impedance tuner can be used at the input of wireless devices in order to provide a significantly broader bandwidth or to reconfigure the impedance match spectrum. The tuner uses a microstrip loaded-line circuit topology with multiple stubs that each have a varactor diode located at the end. The results show that the tuner can achieve a broadband impedance match for a wide variety of loads that are either purely resistive or that have a large reactance as well.**

***Index Terms*—Automatic match control (AMC), intelligent RF front ends, reconfigurable tuner.**

I. Introduction

THE bandwidth of many wireless devices is governed by the input impedance of the antennas or by the impedance match between devices at the RF front end. This imposes severe design constraints as the antenna must both be an efficient radiator to free space, yet provide an appropriate impedance match to the front-end circuits. Simple and small antennas are bandwidth limited, while broadband antennas are typically electrically large (at the highest frequency of interest) and require careful design to fit on portable devices. The input reactance of the antenna, in general, varies with frequency more than does the input resistance of the antenna [1]. Tuning a complex impedance to a purely real impedance, such as a transmission line over a broad frequency band is difficult. An automatic match control (AMC) circuit placed between the antenna and the RF circuits will significantly increase the bandwidth or allow reconfiguration of the spectral mask of accepted and rejected signals. The AMC consists of a broadband RF impedance tuner, a reflection coefficient sensor, and a biasing circuit, as shown in Fig. 1. The AMC can be used with low-cost and low-profile antennas; may be used to correct for high mismatch effects at the input and output of power amplifiers, which could improve power added efficiency and the bandwidth of the amplifier; and can be used for reconfigurable RF systems, where it is important to dynamically reconfigure the spectral mask of the input match as a function of frequency. The AMC can be used to correct for real-time changes in the antenna input impedance in the case where the user places a hand over the antenna during operation and thus significantly changes the reactive impedance [2]. In this paper, we present our results on the design and development of the reconfigurable RF impedance tuner.

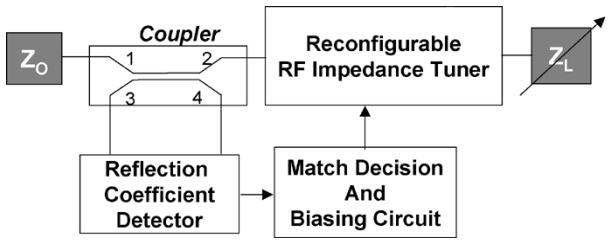

Fig. 1. Block diagram of automatic match control system.

The design of tunable front-end filters has been considered for many years. Varactor and PIN diodes were used in much of the earlier work. Some examples of these are discussed in [3] and [4]. The majority of tunable filters were aimed at the tuning center frequency and bandwidth of operation while assuming a 50-Ω load impedance. A reconfigurable bandpass filter with combination of varactor diodes and ring resonators is presented in [3]. Their research showed that ring resonators have the potential to provide very good passband properties and are easily tuned without the need to shunt the tuning element to ground. This work indicates the advantages of using coupling between resonating elements to increase the bandwidth. Their research mentioned altered coupling between resonators, but a circuit using this information was not designed.

Recent work in reconfigurable matching networks has involved circuit topologies with RF microelectromechanical systems (MEMS) switches or capacitive devices [5]–[11]. RF MEMS are inherently low loss and are compatible with high frequency fabrication methods. Most of the matching networks that involve RF MEMS operate at relatively high frequencies (10–20 GHz) or must be integrated with fixed capacitors for lower frequency operation. A double-stub impedance matching network using MEMS as discussed in [5], [6] can be configured to match a fairly wide range of loads over about a 10%–15% bandwidth in the 10–20-GHz frequency range. Impedance tuning is accomplished by capacitively loading the stubs by a bank of capacitors using MEMS switches. This approach allows a discrete set of loads to be matched. Additional load cases, require additional capacitors and switches. A similar approach is presented in [7] to design a matching network for power amplifiers. They showed that the efficiency of power amplifiers can be improved from reconfigurable input and output matching circuits. The loads that are matched in this work; however, are only slightly reactive, and the double-stub tuner is rather narrowband. In [8], an RF MEMs-based tunable filter using *LC* resonators for 110 MHz to 2.8 GHz was developed.

Manuscript received February 15, 2005; revised July 21, 2005. This work was supported by the National Science Foundation under Grant EEC-0333046.

The authors are with Department of Electrical and Computer Engineering, The University of Arizona, Tucson, AZ 85721 USA (e-mail: melde@ece.arizona.edu).

Digital Object Identifier 10.1109/TAP.2005.863396

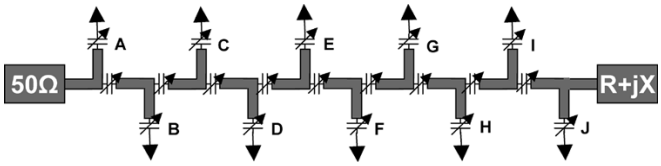

Fig. 2. Ten-stub reconfigurable RF impedance tuner.

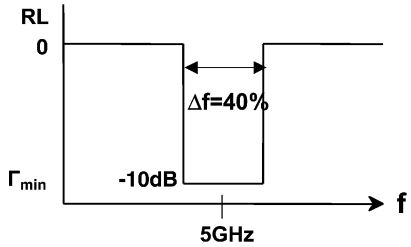

Fig. 3. Desired impedance spectral profile.

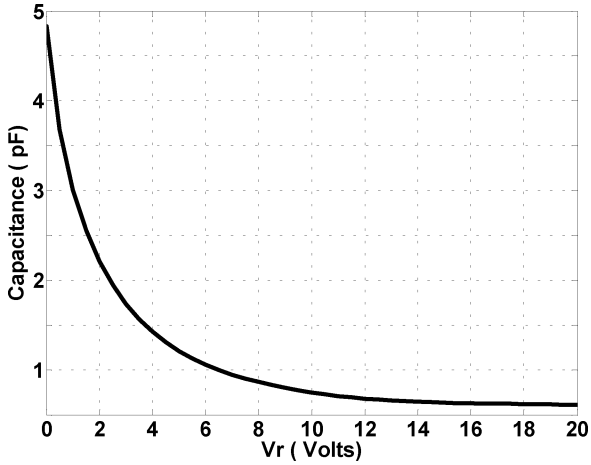

Fig. 4. Capacitance-voltage curve for Microsemi MPV1965 diode.

The filters essentially use a bank of fixed MIM capacitors that are combined in series with RF MEMS switches to create the variable capacitor structures [9]. In the prior work, it was primarily the frequency of operation and the bandwidth that was tuned. A 50-Ω load impedance is assumed. Distributed MEMS transmission lines (DMTL) in coplanar waveguide (CPW) offer a lot of potential for tuning. The objective of DMTLs is to periodically load the CPW to create a slow wave structure that changes the characteristic impedance and the phase velocity. The DMTL resonators discussed in [10] show a narrowband tuning range at 20 GHz.

A complete intelligent high frequency front-end system that operates at 390 MHz is presented in [12]. A simple impedance matching network using *LC* resonators is connected to a coupler that detects a mismatch and a control circuit is used. Due to the relatively low frequency of this system, a microstrip coupler with good isolation is obtainable and a lumped element approach to the tuner was used. The impedance matching network uses a discrete tuning method with PIN diodes. The impedance matching network operates at a relatively low frequency, is generally narrowband, and matches for a discrete set of loads. This paper primarily focuses on comprehensive descriptions of the impedance control and correction algorithms. This paper represents one of the first instances where the complete picture of an intelligent RF control system was presented with the goal of impedance matching.

In the present paper, we present the design and the development of a broadband RF impedance tuner. The tuner is based upon a microstrip loaded-line type topology with varactor diodes at the end of the stubs and between resonator sections as shown in Fig. 2. Multiple resonators are used to satisfy the wide instantaneous bandwidth requirement. Microstrip is used since it allows convenient implementation of the necessary dc control lines, blocking capacitors and inductors. Varactor diodes are used because of their wide usage as tuning elements in the RF frequency range and their relative ease in developing a prototype to validate the design approach. The loaded-line topology is well known for phase shifter applications. The work presented here can be extended to circuits with low loss microwave MEMS capacitive tuning elements as well. The RF impedance tuner in this case can match a continuous range of loads.

The RF impedance tuner has been designed and simulated extensively, fabricated in microstrip, and tested. In this work we demonstrate the outstanding tuning performance of the circuit and describe the design approach used to develop the circuit. This approach may be used to design similar circuits at other frequencies or with other tuning devices. We present a new statistical cost function used to optimize the overall tuner design and diode settings for a broadband impedance match.

Section II discusses the design approach for the reconfigurable RF impedance tuner. Section III describes the simulation and optimization of the impedance matching network for a wide variety of loads. Section IV discusses the circuit fabrication and compares simulation results to measurements on a prototype circuit. This section also reports the power handling capability of the tuner. Section V presents results that show the capability of the RF impedance tuner to provide alternative impedance match spectrums, and Section VI presents some conclusions.

II. Reconfigurable Tuner Design

The goal of the tunable matching network in this paper is to provide wide instantaneous bandwidth (at least 40%) at a 5-GHz center frequency and be tunable to function with wide bandwidth for a diverse set of load conditions. The tuner uses a loaded-line topology as shown in Fig. 2. Fig. 3 shows the desired impedance spectral profile of the tuner. Varactor diodes were chosen for this work because of their ability to provide continuous tuning, their wide availability, and their ease of implementation in fabrication of a prototype design. Although varactor diodes have more loss than MEMS devices, they were used in this case primarily to demonstrate the S_{11} tuning aspects of the structure. The diode is a MPV1965 [13] and has a useable capacitance range that spans from 0.2 to 5 pF, with a nominal capacitance of 3.5 pF. The Q factor of the diode is 1500, and the series resistance is about 1 Ω. The capacitance-voltage curve for this diode is shown in Fig. 4. In this design, we presume the design to be manufactured on Rogers Corporation Duriod 6006 with $\varepsilon_r = 6.15$, a dielectric thickness of 25 mils., a loss tangent of 0.0027, and 1 oz. rolled copper.

Implementation of an impedance matching network can be accomplished using a variety of methods. Transformers or periodic structures such as filters are often used [14]. In general, impedance matching networks are designed specifically to match a set of source and load impedances, Z_0 and Z_L, that are constant and do not vary with frequency. In practice, it is not uncommon that the source and load impedances not only vary with frequency, but often vary at a fixed frequency.

Fig. 2 shows a layout of the microstrip topology used for the circuit. Ten stubs were used in order to achieve the 40% bandwidth goal. Varactor diodes are placed at the end of each stub and on the interconnecting microstrip lines. The design process is as follows.

1) Synthesize the impedance matching network analytically using filter theory and coupled resonators. This design is referred to as the 50-50 design since the source and load impedances are both set to 50 Ω. This step determines the impedance of the stubs and the interconnecting lines. The actual impedance values depend upon the number of stubs and the desired fractional bandwidth of the tuner. This step is described in Section II-A.

2) Once the impedance of the stubs and interconnecting lines are determined, they are converted to microstrip and modified to account for the added diode capacitance. This step is discussed in Section II-B.

3) The design is then refined by optimizing the microstrip 50-50 design with the varactor diodes to obtain all of the fixed microstrip dimensions. This step determines the final lengths and widths of the microstrip for each section. Agilent advanced design system (ADS) [15] was used for this work. Practical parameters such as microstrip bends, vias, etc. can be included in the optimization. A unique cost function is used to obtain the best design. In this step, all of the varactors are set their nominal capacitance value. This step is discussed in Section III.

4) The diode settings for various non–50-Ω load cases are determined by using optimization in ADS, to determine the capacitance values of the varactor diodes. In this step, all of the microstrip dimensions are fixed and only the capacitance values are allowed to vary.

A. Chebyshev Bandpass Filter Synthesis of 50-50 Design

In this step, the impedances of the different filter sections are determined using an analytical filter synthesis technique. A Chebyshev bandpass filter response was chosen since the Chebyshev response gives the broadest bandwidth with the fewest number of sections [14]. The desired response has a very small ripple in the passband and a steep slope in the transition region between the passband and stopband. The procedure for determining the low-pass prototype for a Chebyshev response, given a particular passband ripple is well documented in [14] and [16]. The admittances (and, thus, impedances) of the various sections are determined by using the design process described in [16, Table 10.03–1] for synthesizing the filters using using coupled resonators given the Chebyshev coefficients for a low-pass prototype filter. The specific approach uses the design equations for filters with shunt quarter-wavelength stubs and quarter-wavelength interconnecting lines. The diodes are not considered in this step. In the next step, the filter design is slightly modified to include the diodes. The number of sections needed to obtain the desired passband response is determined by the center frequency, the bandwidth, and the desired passband return loss. In the design equations given in [16] there is a dimensionless constant, d, that may be chosen to adjust the impedance levels for the filter sections. A 40% bandwidth filter, centered at 5 GHz with a 0.05- dB passband ripple and a 15-dB passband return loss resulted in a ten-stub tuner. A 15-dB return loss was specified in order to ensure that a maximum of 10-dB return loss is obtained in the final tuner when practical microstrip elements are included. This step determines all of the impedances for the stubs and interconnecting lines given a 50-Ω source and load.

TABLE I
STUB IMPEDANCES AND MICROSTRIP DIMENSIONS FOR TEN STUB IMPEDANCE TUNER

n	A	B	C	D	E
Z_i (Ω)	22.1	11.1	11.0	10.8	10.8
Z_i+Z_{var} (Ω)	23.8	14.2	14.1	14.0	14.0
Width [mils]	124	290	293	300	300
Length [mils]	262	251	251	250	250

B. Design Modification for Microstrip Implementation and Diode Inclusion

Once the impedance values for the different sections are known it is straightforward to convert them to microstrip lengths and widths using microstrip physical circuit design equations [14]. Varactor diodes are positioned at the end of each stub and on the interconnecting lines. In order to insure that the desired Chebyshev filter response is maintained in the 50-50 design *after* adding the diodes, the magnitude of the impedance of the microstrip stub with varactor must be slightly modified so that it is equal to the calculated stub impedance determined from the first step. The impedance of the varactor is computed at the center frequency of the passband. The varactor in this case has a nominal capacitance of 3.5 pF at 5 GHz, and the resulting diode reactance is $X_C = 1/j2\pi fC$ or $-\text{j}9.10\,\Omega$. The impedance of a transmission line is the sum of the real and reactive parts. The magnitude of the impedance can be used to obtain the value, R, which is the impedance of the microstrip line using

$$|Z| = \sqrt{R^2 + (X_L - X_C)^2}. \tag{1}$$

The diode is assumed to be purely capacitive, and thus X_L is set to zero. In order to avoid a large step between the real impedance of the microstrip line and the reactive impedance of the varactor, the condition that these impedances be within 15 Ω from one another was enforced, so that

$$|R_c - X_c| < 15\,\Omega. \tag{2}$$

Table I shows the calculated impedances and microstrip dimensions for each quarter-wave shunt stub and Table II shows the impedances and microstrip dimensions for each interconnecting line for the ten-stub 50-50 design. The tables list the initial calculated impedances and the modified impedances based on loading with a varactor diode. In order to reduce the number

TABLE II
INTERCONNECT IMPEDANCES AND MICROSTRIP DIMENSIONS FOR TEN STUB IMPEDANCE TUNER

N,n+1	A,B	B,C	C,D	D,E	E,F
$Z_{i,i+1}$ (Ω)	41.7	40.8	43.7	44.6	44.9
$Z_{i,i+1}+Z_{var}$ (Ω)	42.6	41.8	44.6	45.5	45.8
Width [mils]	49	51	45	43	43
Length [mils]	277	277	278	279	279

of variables used in the subsequent optimization steps, symmetry about the center of the tuner is imposed. In Fig. 2, for example, the length and width of microstrip stubs A and J are identical to one another, the length and width of microstrip stubs B and I are identical to one another, and so on. Symmetry was also imposed on the interconnecting lines as well so that the separation between stubs A and B (A, B) is the same as the separation between stubs I and J (I, J). Symmetry was not imposed on the diode settings.

III. SIMULATION AND OPTIMIZATION

The final design of the tuner involves simulation and optimization of the tuner using ADS. The optimization requires specifying a starting design, the design parameters to be adjusted, an optimization type, and an optimization cost function (or goal) that specifies the final tuner performance goals. The microstrip lengths and widths reported in Tables I and II were used along with structural elements such as microstrip bends, tees, and gaps as the starting design for the optimization. This approach anticipates that the tuner design obtained from analysis only needs slight corrections for optimal performance. The cost function must be carefully specified in order to maximize the performance of the tuner with as few resonators as possible.

The first optimization task is the third step in the overall design process and involves finding the optimal length and width dimensions for all of the microstrip lines for the 50-50 design. All of the varactors in this case are set to their nominal state capacitance of 3.5 pF and the source and load impedance values are fixed at 50 Ω. In this case, only the microstrip dimensions are allowed to vary and the varactor settings remain fixed throughout the optimization. The final design resulting from this step is used to generate the masks for etching the microstrip tuner.

Initially, a simple cost function that enforces S_{11} to be below -10 dB at each individual sampled frequency in the 4.5 GHz to 6.5 GHz passband was used. The approach had minimal effectiveness and often produced designs that satisfied most of the optimization criteria, yet had several frequency points above -10 dB. The 40% bandwidth goal was not achieved with this cost function, and the Chebyshev type passband response obtained from the first step in the process was not maintained.

A new cost function that considers the frequency response in the passband as an entire set of points (i.e., a function) was developed. The development of this cost function was a significant factor in successfully designing and evaluating the RF impedance tuner. The values of S_{11} in the passband were treated as a *statistical* cost function, rather than individual values. The statistical function generates a score that was used to evaluate the performance. The cost function was specifically developed to score the performance against the desired case shown in Fig. 3. Fig. 3 satisfies the Bode-Fano matching limit [17], by maximizing the S_{11} bandwidth without any extremely low return loss values in the passband. The optimum S_{11} response has a symmetric Chebyshev response with very little ripple in the passband. The ADS optimization block allows the user to specify a series of equations to express the optimization cost function and thus facilitates the development of unique cost functions that can be tailored for the design problem.

The statistical cost function has the form

$$\text{Cost} = a \cdot |\mu| - b \cdot \left(\frac{\sum_{i=1}^{N} \left(|S_{11_i}| - |\mu|\right)^4}{N\sigma^4} - 3 \right) - c \cdot \left(\frac{\sum_{i=1}^{N} \left(|S_{11_i}| - |\mu|\right)^3}{N\sigma^3} \right) - \text{penalty} \quad (3)$$

where μ is the mean value of the return loss in the passband, and σ is the standard deviation of the return loss in the passband. The values specified for a, b, and c are constants used to weight the importance of either the first, second, or third term in (3) on the overall score. The numerators in each of the second and third terms in (3) include a sum over N values of S_{11} that are in the passband from 4.5 to 6.5 GHz. The cost function in (3) is a maximizing cost function, which means that the best design is obtained when the score given by (3) is maximized.

The key parameters for the optimal S_{11} response are the mean value, the flatness, and the symmetry around the center frequency. The first term in (3) specifies the mean value of the return loss. A low average return loss of all of the points in the passband results in a large number for this term. The second term in (3) determines the flatness of the return loss in the passband. The flatness is determined by the Kurtosis of a function [18]. The value of the Kurtosis is based upon the size of the tails (at either end) of a function. The Kurtosis of a normal distribution is zero. It is assumed in this case, that a nonzero Kurtosis value reduces the score of the cost function and, thus, should be subtracted in (3). The third term in (3) determines the symmetry of return loss in the passband. The symmetry is evaluated by the Skewness of a function [18]. A symmetrical passband has zero Skewness. If the function is skewed to the right or left, the Skewness is positive or negative, respectively. In (3), any nonzero value of Skewness reduces the score of the cost function and, thus, this term is subtracted from (3).

In order to significantly reduce the occurrence of any value of S_{11} in the passband to creep above -10 dB, a *penalty* number is included to the cost function in (3). The inclusion of this *penalty* parameter in this manner resulted in the broadband final designs, since the cost function score was severely penalized when any value of S_{11} in the passband is above -10 dB. The constants a, b, and c were determined so that a cost function score of 100 or larger is considered good. The value of *penalty* was set to 90.

To implement the cost function in ADS, the value of S_{11} for the 200 frequency points between 4.5 and 6.5 GHz are stored in a matrix. The mean value and standard deviation of these values

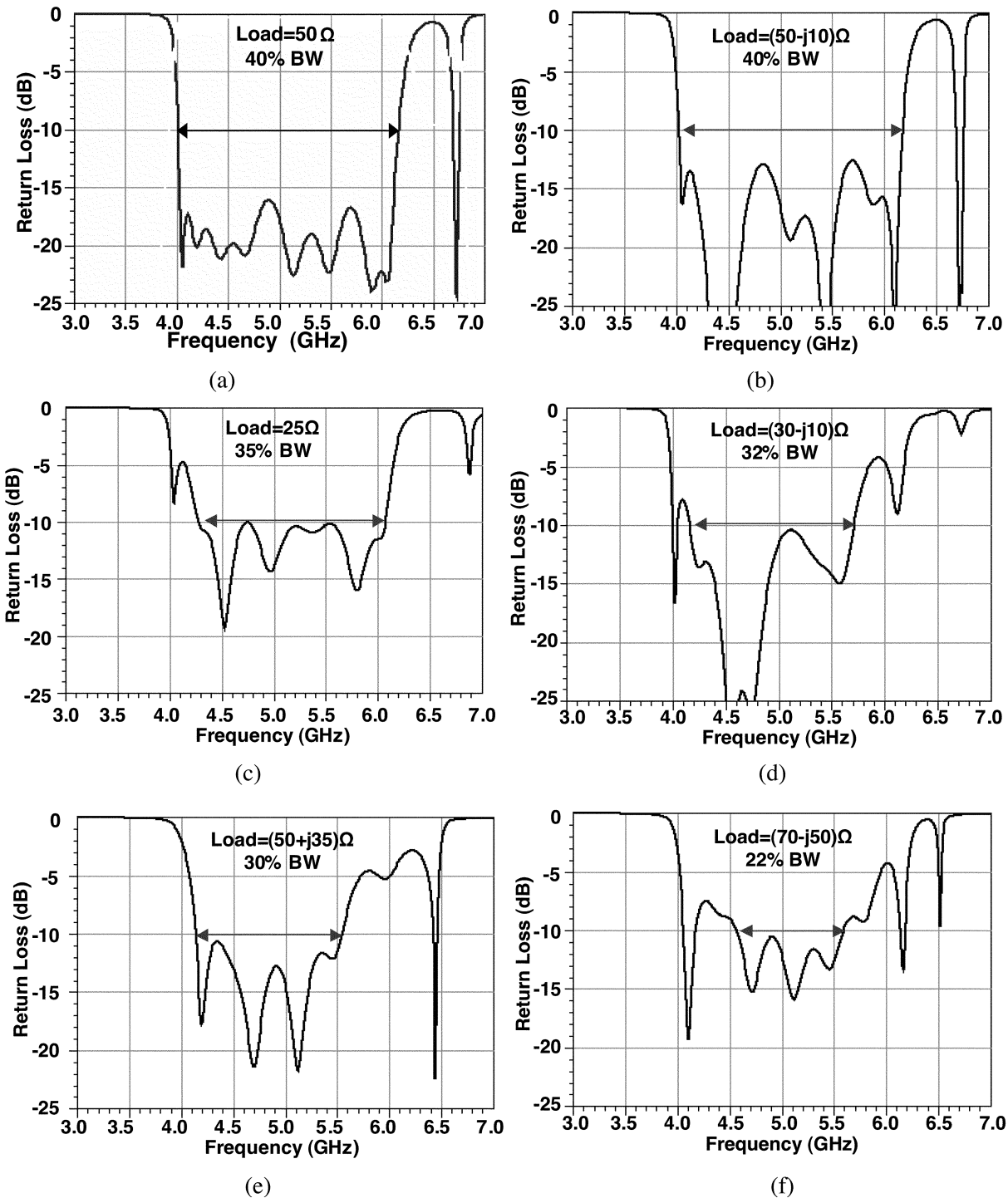

Fig. 5. Return loss of ten-stub microstrip tuner for different load impedances.

is then computed. These are used to compute the cost function given in (3). The ADS optimizer then works to modify the design. Random optimization was used, although the Gradient Search and Quasi-Newton methods were tried as well. The random optimizer only took about 10 min from start to finish, while the other methods took nearly one hour. The proposed process uses the analytical design as the starting design, yet our results found that the random optimizer was not especially sensitive to the starting design and converged to the same final solution. The other two optimizers were sensitive to the starting design.

The final step in the tuner design is to determine the diode capacitance settings for different non-50 Ω load cases. In this step, all of the microstrip dimensions are fixed, the input impedance is set to 50 Ω, the load impedance is set to $\mathrm{R}+\mathrm{jX}$, and the values of the diode capacitances are determined by ADS optimization using the cost function given in (3). In each case, the diodes are set to 3.5 pF for the starting design, and random optimization is used to determine the final values needed to achieve broadband performance. Each optimization takes about 10 min from start to finish in these cases as well.

TABLE III
DIODE CAPACITANCE (PF) SETTINGS FOR DIODES ON STUBS FOR TEN-STUB IMPEDANCE TUNER

Load	A	B	C	D	E	F	G	H	I	J
50-j10	3.5	3.5	3.5	3.5	3.5	3.5	3.5	3.5	3.5	3.5
30-j10	1.34	3.59	1.40	5.68	3.68	2.59	3.89	2.06	2.33	4.78
50+j35	4.42	1.27	2.46	0.832	4.85	2.47	3.96	5.01	3.70	3.89
70-j50	5.02	0.58	2.41	4.84	2.75	2.73	3.51	4.54	5.23	3.50

TABLE IV
DIODE CAPACITANCE (PF) SETTINGS FOR DIODES ON INTERCONNECTING LINES FOR TEN-STUB IMPEDANCE TUNER

Load	A,B	B,C	C,D	D,E	E,F	F,G	G,H	H,I	I,J
50-j10	3.5	3.5	3.5	3.5	3.5	3.5	3.5	3.5	3.5
30-j10	2.82	5.71	4.58	1.61	3.57	3.42	3.92	5.66	1.27
50+j35	5.21	1.12	3.41	2.24	1.01	5.15	3.59	3.69	2.98
70-j50	0.50	5.18	3.64	1.43	3.96	4.29	2.62	2.64	4.93

TABLE V
MICROSTRIP DIMENSIONS FOR THREE STUB IMPEDANCE TUNER

Stub/Interconnect	A	B	A,B
Width [mils]	116	157	42
Length [mils]	281	294	175

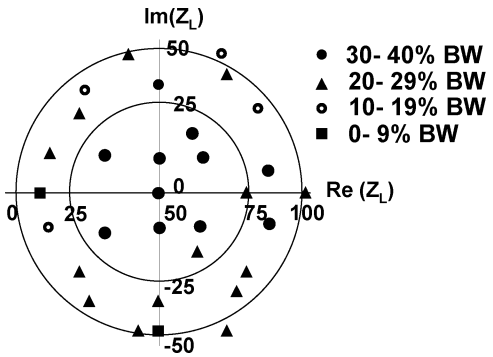

Fig. 6. Bandwidth of ten-stub impedance tuner for different load impedances.

Fig. 5 shows the return loss of the ten-stub RF impedance tuner for several load impedance cases. The percentage bandwidth indicated in these plots is determined by the frequency band which has *consecutive* return loss values below -10 dB. Fig. 5(a) shows that the 50-50 design has a 40% frequency bandwidth. Tables III and IV show the capacitance settings of the diodes for the non-50 Ω load cases. These tables show that in some cases, the capacitance of the diodes is slightly above 5 pF. Fig. 6 shows the instantaneous bandwidth computed for the 10-stub tuner for many different load cases. The horizontal axis is the real part of the load impedance and the vertical axis is imaginary part of the load impedance. These figures clearly show the potential of the tuner to match to a diverse set of loads, even with high reactance. Fig. 6 shows the difficulty of achieving wide instantaneous bandwidth when the reactance is high. Loads that are nonreactive or only slightly reactive can be matched over a wide instantaneous bandwidth. It is more difficult to achieve wide bandwidth with loads that are highly reactive.

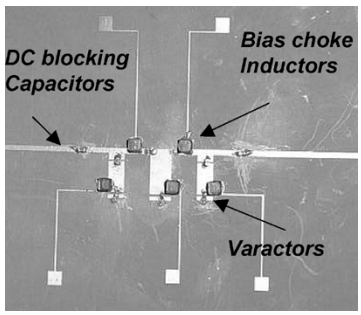

Fig. 7. Photograph of three-stub RF impedance tuner.

IV. MEASUREMENT VERIFICATION ON THREE-STUB PROTOTYPE

To verify the circuit design and simulation approach, a prototype three-stub bandwidth reconfigurable tuner with 30% bandwidth was designed, fabricated, and tested. A three-stub prototype tuner was specifically used to validate the design process, refine the ADS models to include diode parasitics, and to evaluate the implementation details associated with tuner fabrication and operation. The three-stub tuner utilizes five diodes and the associated bias lines, whereas the ten-stub tuner utilizes 19 diodes and the associated bias lines. A three-stub tuner was used as the prototype because it is simpler and quicker to fabricate than the ten-stub tuner, yet provides enough elements in order to yield interesting frequency characteristics and to ascertain fabrication and performance issues. Table V lists the final microstrip dimensions of the stubs and interconnecting lines for the three-stub tuner.

The goal is to simulate a three-stub tuner while taking into account as many physical properties as possible, and then to compare the simulated results with measured results. Fabrication of the impedance matching network took place at the University of Arizona Microelectronics Laboratory. The structure was fabricated on Rogers Corp. Duroid 6006. Fig. 7 shows a photograph of the three-stub tuner. This figure shows the tuner structure and the dc blocking capactors. Very thin, high impedance conductors were used as bias lines. Chip inductors were used to isolate the bias lines from the RF signal path. The overall length of this structure on a material of $\varepsilon_{\rm r} = 6.15$ is approximately 1100 mils. A coaxial double-stub tuner was used to create the mismatched load cases for the measurements. The load characteristics of the double-stub tuner can be carefully controlled by lengthening or shortening the two coaxial lines.

Fig. 8 compares the measured and simulated results of the three-stub tuner for several different load cases. The load impedance in Fig. 8(a) is 50 Ω and does not vary with frequency. The load impedances in Fig. 8(b)–(d) are $50 + {\rm j}50\ \Omega$, $60 + {\rm j}21\ \Omega$, and $40 + {\rm j}50\ \Omega$ respectively, at 5 GHz. In these cases, the load impedance varies with frequency. The load impedance of the measured results varies as a function of frequency because of the double-stub tuner that is used to create the mismatched loads. The frequency dependent S_{11} of the double-stub tuner configured for each different load was measured. These values were used to create a frequency dependent single port termination dataset for each different load. These datasets were used in ADS in order to simulate the

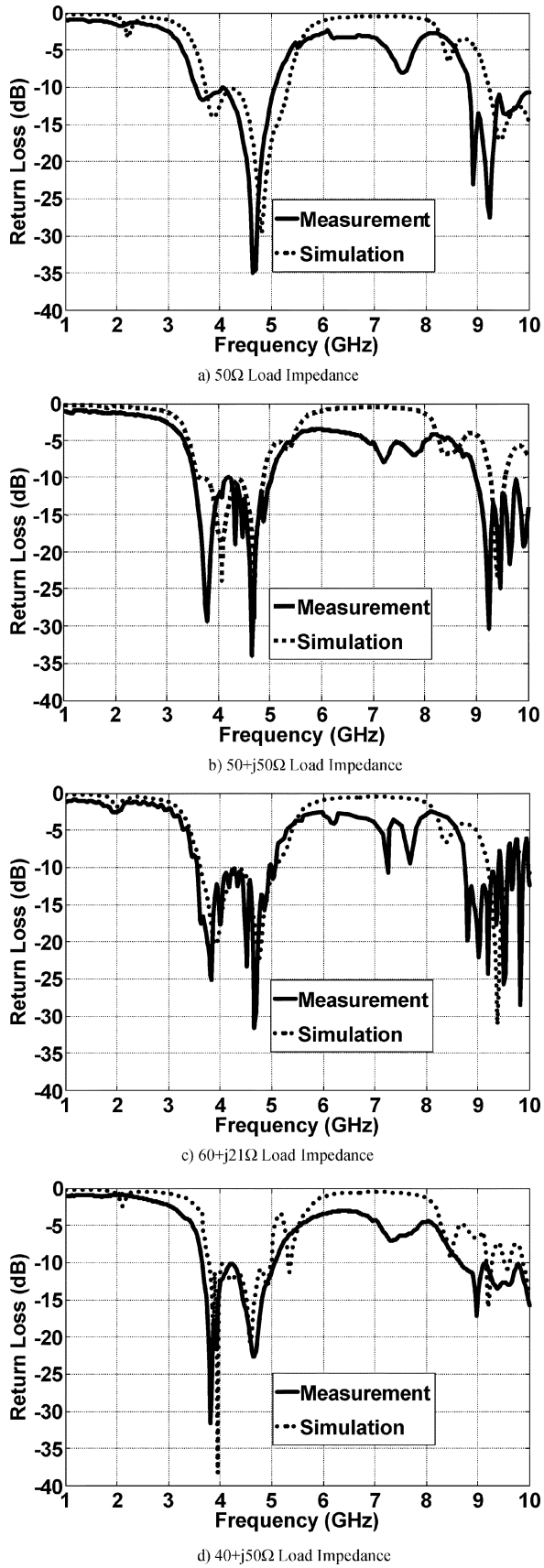

Fig. 8. Comparison of measured and simulated results for three-stub tuner.

tuner performance with the appropriate frequency dependent load behavior for comparison to measurement.

Fig. 8 shows a good comparison between the measured and simulation results for a variety of different load cases. The measured results on the three-stub tuner with a 50-Ω load were used to determine the parasitics of the varactors. The parastic values were determined by matching the simulation and measured results in Fig. 8(a). Once the parasitic values were determined, they were directly used in the ADS simulations shown in all the cases in Fig. 8 For the 50 Ω load, the simulation data predicts a 36.5% bandwidth where S_{11} is less than -10 dB, while the measured data shows a 35% bandwidth. The simulation results in Fig. 8(b) predict a 31% bandwidth, while measurements show 33.3% bandwidth. For the $60 + j21\,\Omega$ load, simulations predict a 32.65% bandwidth and measurements give a 34.47% bandwidth. The bandwidth for the simulation results in Fig. 8(d) is 28.2% and the bandwidth for the measured results is 32%. Very good agreement between the measured and simulated results was obtained using this approach for a variety of different load cases. These results show that the design approach and ADS simulation model with the frequency dependent load and the diode parasitics can effectively be used for obtaining a reconfigurable tuner design.

The insertion loss of the tuner with each diode biased to their nominal state of 3.5 pF is -11 dB at 4.8 GHz, which is rather high. The diode settings correspond to the 50-Ω load case. Fig. 8(a) shows that at 4.8 GHz, the tuner is well matched, so this loss is primarily due to the resistive loss in the diodes. The diodes that are placed on the interconnecting lines contribute the most loss, since they reside directly on the microstrip signal line rather than on one of the stubs. The MPV1965 diode was primarily chosen for its tuning range over the frequency band of interest. Loss was not a constraint in the original design process described here. The measured results on the prototype indicate that design process and optimization cost function should be refined to include low insertion loss as a design parameter. The insertion loss can be reduced by using one or more approaches that include, selecting a varactor with much lower series resistance, replacing the varactors with very loss-loss microwave MEMS devices, or by redesigning the tuner without diodes in the interconnecting microstrip signal lines.

The power handling capability of the three-stub tuner was also measured. The diodes were biased to their nominal state (i.e., the 50-50 configuration) and the input power into the tuner was varied from 0 to 14 dBm. Fig. 9 shows the measured S_{11} as a function of frequency measured for an input power of 0, 10, and 14 dBm. Fig. 9(a) shows the S_{11} magnitude and Fig. 9(b) shows the S_{11} phase. These plots show that over the range from 0 to 14 dBm, there is little change to the match of the tuner. The insertion loss as function of input power for input power levels ranging from 0 to 16 dBm at 4, 5, and 6 GHz was also measured. These results also show no change in the insertion loss over the input power ranges.

V. Alternative Spectral Profiles

Simulations of the ten-stub tuner were used to explore the potential for reconfiguring the impedance spectral profile. Fig. 10 shows the results of ADS simulations on the ten-stub tuner using a spectral impedance profile that gives a dual-band (dual-notch) impedance matching response. This was obtained using the statistical cost function, yet defining it for two narrow frequency

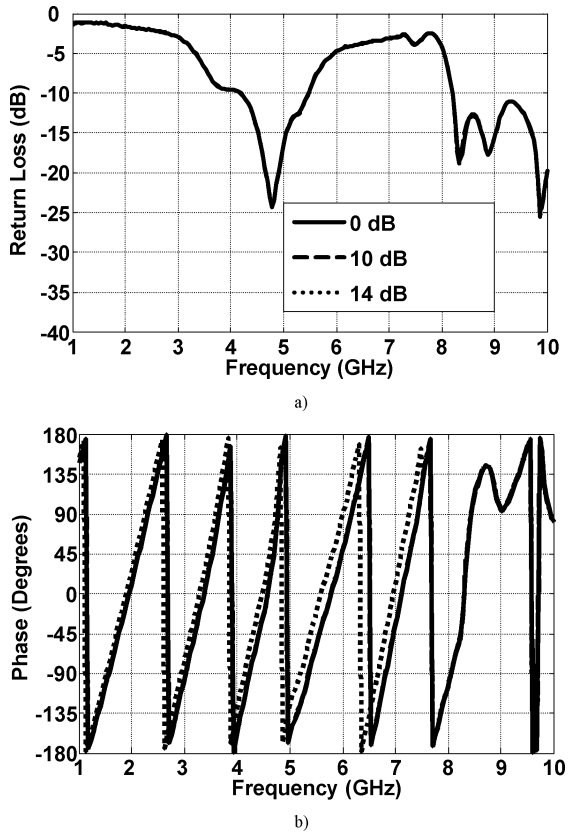

Fig. 9. Comparison of S_{11} for different input power levels on three-stub tuner with 50 Ω load.

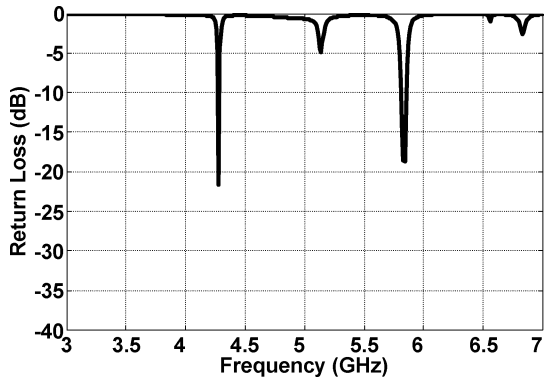

Fig. 10. Simulated dual-band response for ten-stub tuner.

bands. The load impedance in this case was set to 50 Ω. To achieve this result, the varactor diodes were allowed to have capacitance values outside their specified range. This result indicates that the ten-stub tuner has the capability to achieve alternative spectral profiles if it is combined with tuning devices with a much larger range of capacitance values.

VI. Conclusion

The design and synthesis of a wideband dynamically reconfigurable RF impedance tuner that could be used for an automatic match control system has been presented. The design of the tuner was based on well-established microwave methods that have been adapted and developed to add properties of the tuning devices to allow reconfiguration for different load conditions and impedance spectral profiles. A new statistical optimization cost function has been proposed in determining the quality of an impedance matching network. This cost function also optimized the performance of the reconfigurable matching network by using the synthesized structure as a starting point. The reconfigurable impedance matching network has been simulated, fabricated and tested and has been shown to have a broadband impedance match a continuous range of loads.

References

[1] K. L. Virga and Y. Rahmat-Samii, "Low-profile enhanced-bandwidth PIFA antennas for wireless communications packaging," *IEEE Trans. Microw. Theory Tech.*, vol. 45, pp. 1879–1888, Oct. 1997.
[2] M. A. Jensen and Y. Rahmat-Samii, "EM interaction of handset antennas and a human in personal communications," *Proc. IEEE*, vol. 83, pp. 7–11, Jan. 1995.
[3] I. C. Hunter and J. D. Rhodes, "Electronically tunable microwave bandpass filters," *IEEE Trans. Microw. Theory Tech.*, vol. MTT-30, no. 9, pp. 1361–1367, Sep. 1982.
[4] M. Makimoto and M. Sagawa, "Varactor tuned bandpass filters using microstrip-line ring resonators," in *IEEE MTT-S Dig.*, 1986, pp. 411–414.
[5] J. Papapolymerou, K. Lange, C. Goldsmith, A. Malczewski, and J. Kleber, "Reconfigurable double-stub tuners using MEMS switches for intelligent RF front-ends," *IEEE Trans. Microw. Theory Tech.*, vol. 51, no. 1, pp. 271–278, Jan. 2003.
[6] K. Lange, "A dynamically reconfigurable impedance tuner using RF MEMS switches," M.S. thesis, Univ. Arizona, Dept. Elect. Comput. Eng., Tucson, AZ, 2001.
[7] Y. Lu, D. Peroulis, S. Mohammadi, and L. Katehi, "A MEMS reconfigurable matching network for a class AB amplifier," *IEEE Microw. Wireless Compon. Lett.*, vol. 13, pp. 437–439, Oct. 2003.
[8] J. Brank, Z. J. Yao, M. Eberly, A. Malczewski, K. Varian, and C. L. Goldsmith, "RF MEMS-based tunable filters," *Int. J. RF Microw. CAE*, vol. 11, no. 5, pp. 276–284, Sep. 2001.
[9] C. L. Goldsmith, A. Malczewski, Z. J. Yao, S. Chen, J. Ehmke, and D. Hinzel, "RF MEMS variable capacitors for tunable filters," *Int. J. RF Microw. CAE*, vol. 9, no. 4, pp. 362–374, Jul. 1999.
[10] Y. Liu, A. Borgioli, A. S. Nagra, and R. York, "Distributed MEMS transmission lines for tunable filter applications," *Int. J. RF Microw.*, vol. CAE 11, pp. 254–260, 2001.
[11] A. Pothier, J.-C. Orlianges, G. Zheng, C. Champeaux, A. Catherinot, D. Cros, P. Blondy, and J. Papapolymerou, "Low-loss 2-bit tunable bandpass filters using MEMS DC contact switches," *IEEE Trans. Microw. Theory Tech.*, vol. 53, no. 1, pp. 354–360, Jan. 2005.
[12] J. Mingo, A. Valdovinos, A. Crespo, D. Navarro, and P. Garcia, "An RF electronically controlled impedance tuning network design and its application to an antenna input impedance automatic matching system," *IEEE Trans. Microw. Theory Tech.*, vol. 52, no. 2, pp. 489–497, Feb. 2004.
[13]. [Online]. Available: www.microsemi.com
[14] D. Pozar, *Microwave Engineering*. New York: Wiley, 2001.
[15] Agilent Advanced Design System (ADS) [Online]. Available: www.agilent.com
[16] G. L. Matthaei, L. Young, and E. M. T. Jones, *Microwave Filters, Impedance-Matching Networks, and Coupling Structures*. Dedham, MA: Artech House , 1980.
[17] R. M. Fano, "Theoretical limitations on the broad-band matching of arbitrary impedances," *J. Franklin Inst.*, vol. 249, pp. 57–83, Jan. 1950.
[18] Hyperstat Online Reference [Online]. Available: http://davidmlane.com/hyperstat/index.html

Richard B. Whatley received the M.S.E.E. degree from The University of Arizona, Tuscon, in August 2004.

Since 2004, he has been with the Jet Propulsion Laboratory, Pasadena, CA. His areas of interest are RF circuit design and high-power solid-state power amplifier design.

Zhen Zhou received the M.S. degree in mechanical engineering from Chongqing University, Chongqing, China, in 1991.

She is currently working toward the M.S. degree in electrical engineering from The University of Arizona, Tuscon, under the guidance of Dr. K. Melde. Her research interest is in automatic control reconfigurable matching networks. She worked for four years in various projects funded by the Chinese Navy, and also for several companies in the U.S., including Nokia, as an RF Design and Test Engineer.

Ms. Zhou was one of the First Prize Winners for technology improvement from the Ministry of Science and Technology of The People's Republic of China, in 1994.

Kathleen L. Melde (previously Kathleen L. Virga) (S'85–M'87–SM'97) received the B.S. degree from California State University, Long Beach, in 1985, the M.S. degree from California State University, Northridge, in 1987, and the Ph.D. degree from the University of California, Los Angeles (UCLA) in 1996, all in electrical engineering. Her dissertation involved the modeling of broadband and integrated antennas for wireless communications.

She is an Associate Professor with the Electrical and Computer Engineering Department, The University of Arizona, Tuscon. From 1985 to 1996, she was with the Radar Systems Group, Hughes Electronics, El Segundo, CA. Her work experience includes diverse projects in the Electromagnetic Systems Laboratory and Solid State Microwave Laboratories of the Radar and Communications Sector. She has made contributions to the design and development of phase shifters, RF feed networks, radiator elements, and transmit/receive (T/R) modules for airborne phased and active array programs. She has extensive experience in modeling, fabrication, and measurement of the performance of antennas, antenna arrays, high-density microwave circuits, and high-speed packaging interconnects. She was a task leader for several internal research and development projects. Her current research interests involve applied electromagnetics, antenna theory and design, and microwave circuit design. Her current projects involve conformal array antennas, antenna element design and characterization, high-speed electronic packaging, and the development of circuits for intelligent RF front ends. She has more than 60 publications and four U.S. patents. She has been an expert witness and consultant in the area of RF circuits and antennas.

Dr. Melde has received numerous awards including the Hughes Aircraft Company Doctoral Fellowship, a UCLA Department of Electrical Engineering Graduate Woman of the Year award, and was a finalist for the URSI Student Competition She has been an invited keynote speaker on several occasions such as the California State University Northridge, School of Engineering commencement, and the Ansoft Corporation's Partner in Design Lectures. She is a member of the Antennas and Propagation (AP-S) and Microwave Theory and Techniques (MTT) Societies. She is a member of the International Radio Science Union (URSI), Eta Kappa Nu, Tau Beta Pi, and Sigma Xi. From 1999 to 2001, she served on the administrative committee (AdCom) for the IEEE AP-S Society. She is an Associate Editor for the IEEE TRANSACTIONS ON ANTENNAS AND PROPAGATION and a Reviewer for several IEEE journals. She is a member of the IEEE AP-S Society Awards committee. She serves on the Technical Program Committee for the annual IEEE International Symposiums on Antennas and Propagation.